

Intermediate structures and their dominant l values in $^{16}\text{O}(^{12}\text{C}, ^8\text{Be})^{20}\text{Ne}$ reactions, $E_{\text{c.m.}} = 11.5$ to 18.6 MeV

J. R. Hurd,* N. R. Fletcher, A. D. Frawley, and J. F. Mateja†

Department of Physics, Florida State University, Tallahassee, Florida 32306

(Received 3 March 1980)

Measurements of $\sigma(\theta, E)$ are reported for $^{16}\text{O}(^{12}\text{C}, ^8\text{Be})^{20}\text{Ne}^*$ reactions to the low lying 0^+ , 2^+ , 4^+ and unresolved 3^- , 1^- final states. The energy range is $E_{\text{c.m.}} \simeq 11.5$ to 18.6 MeV with measurements at ~ 86 keV intervals. Up to 38 angles between $\theta_{\text{c.m.}} = 12^\circ$ and 167° are measured for each energy. A large number of resonances are identified by their appearance over a broad range of forward and backward angles and by their energy correlation over exit channels. Many J^π assignments are inferred from the behavior of back angle $\sigma(\theta)$ across the resonance. All J values are from one to three units less than the optical model grazing angular momentum for the $^{16}\text{O} + ^{12}\text{C}$ channel.

NUCLEAR REACTIONS $^{16}\text{O}(^{12}\text{C}, ^8\text{Be})^{20}\text{Ne}^*$; measured $\sigma(\theta, E)$ to low-lying states for $E_{\text{c.m.}} \simeq 11.6$ – 18.6 MeV and $\theta_{\text{c.m.}} \simeq 12^\circ$ – 167° . Deduced resonant energies and J^π values.

I. INTRODUCTION

Since the first observation of intermediate structure resonances in heavy ion reaction cross sections,¹ interest in the field has steadily increased. However, even with the phenomenal increase in experimental activity in the last few years, there is still a lack of spin information for many resonances and assignments are ambiguous for still others. There is a continuing effort to clarify this picture so that hopefully a unifying explanation of heavy ion resonance phenomena might evolve naturally from a preponderance of high quality data and accurate spin assignments. To date, the only definite result is that simple rotational bands, even though overlapping, do not provide a satisfactory explanation.

The present paper reports cross section measurements for $^{16}\text{O}(^{12}\text{C}, ^8\text{Be})^{20}\text{Ne}^*$ reactions leading to low-lying states of ^{20}Ne . This is an extension to a lower energy range, $E_{\text{c.m.}} = 11.5$ – 18.6 MeV, of work recently reported² for these reactions for $E_{\text{c.m.}} = 18.6$ – 22.7 MeV. The extension is also such that the data cover the entire angular range, enabling us to extract relatively accurate total cross sections. Resonance criteria used are as discussed in the previous publication² with the additional use of these total cross sections. Due to the extent of the project, the present paper is intended only to report the evidence for the intermediate structures, their energies and approximate widths, and their dominant l values whenever possible. Analyses are limited to comparison of back-angle angular distributions with squared Legendre polynomials and the extraction of linear Legendre expansion coefficients for the ground state

angular distributions. Statistical and other reaction model analyses will be presented at a later time. It should be noted, however, that too often such analyses have been used on data so limited that the results are questionable. This will not be the case for the complete measurements presented here.

II. COMMENTS ON EXPERIMENTAL PROCEDURE

Many of the experimental details are sufficiently similar to those in our previous work^{2,3} on ^8Be reactions that only those specifically pertinent to the present experiment are included. One important difference between this and the work of James² is that both carbon and oxygen targets were used in order to obtain measurements of $\sigma(\theta, E)$ over an angular range of $\theta_{\text{c.m.}} \simeq 12^\circ$ – 167° . The angle quoted is always for an oxygen target and a ^{12}C beam, thus the forward angle refers to the direction for maximum alpha-particle transfer cross section, unlike the work of James.

The carbon targets were self-supporting foils of natural carbon. For oxygen targets, vacuum depositions of Fe_2O_3 on ~ 100 $\mu\text{g}/\text{cm}^2$ gold backings were used. The energy loss of beam particles in the carbon foil or the Fe_2O_3 layer was always close to the energy step size (~ 86 keV c.m.) used in measuring excitation functions. Carbon buildup on targets was measured and appropriate corrections were made in the extraction of cross sections from carbon targets and in the determination of energy loss of beam particles for both targets. All resonance energies quoted herein have been corrected for energy loss to the center of the active target. Target thicknesses of ^{12}C , ^{16}O , and

Fe were determined by measuring the Rutherford scattering of ^{16}O particles at $E_L = 20$ MeV and $\theta_L = 20^\circ$ for a known detector geometry.

The kinetic energy spectra of ^8Be (g.s.) particles is formed by adding the energies of kinematically selected coincident alpha particles.^{3,4} A sample spectrum for ^{16}O bombardment of a carbon target at $E_L = 40$ MeV, $\theta_L = 7.5^\circ$ is shown in Fig. 1. Such spectra allow one to extract yields leading to the 0^+ , 2^+ , 4^+ and 3^- , 1^- states of ^{20}Ne with considerable accuracy, thus providing good back-angle data for $^{16}\text{O}(^{12}\text{C}, ^8\text{Be})^{20}\text{Ne}^*$ reactions. Yields to the 2^- state and other higher excited states were not extracted. Forward angle spectra for ^{12}C bombardment of Fe_2O_3 targets are not as attractive. There are no contributions from Fe or Au; however, even a small quantity of ^{12}C contamination produces considerable yield from the $^{12}\text{C}(^{12}\text{C}, ^8\text{Be})^{16}\text{O}^*$ reactions, curtailing the determination of $\sigma(\theta, E)$ to the 4^+ and 3^- , 1^- final states in $^{16}\text{O}(^{12}\text{C}, ^8\text{Be})^{20}\text{Ne}^*$ at low bombarding energies and forward angles.

III. EXPERIMENTAL RESULTS

A. Excitation functions and resonance energies

Excitation functions measured in ~ 86 keV steps from $E_{\text{c.m.}} \approx 11.5$ – 18.6 MeV for $^{16}\text{O}(^{12}\text{C}, ^8\text{Be})^{20}\text{Ne}^*$ reactions leading to the low-lying $J^\pi = 0^+$, 2^+ , and 4^+ states are shown in Figs. 2, 3, 4, respectively. Data were accumulated at 2.5° intervals in the laboratory with the forwardmost angle being 7.5° relative to both ^{12}C and ^{16}O beams. Since the width of the efficiency function³ for ^8Be detection is $\sim 2^\circ$, it is clear that a complete sampling of the angular dependence is obtained, while maintaining sufficient angular resolution not to obscure any details of the angular dependence. The center-of-mass angles indicated in the figures are approxi-

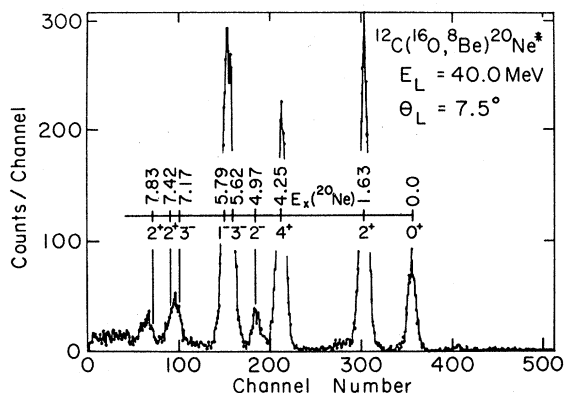


FIG. 1. Energy spectrum of ^8Be particles generated by the addition of energies of alpha particles in appropriate kinematic coincidence.

mate values, not only because of the energy dependence of $\theta_{\text{c.m.}}$ for a fixed θ_L , but also at a few angles near 60° both ^{12}C target data and ^{16}O target data are included in the same excitation function and of course the energy shifts in $\theta_{\text{c.m.}}$ are thereby of opposite sign. There are several small regions of missing data due to experimental limitations. In Fig. 2 excitation functions at $\theta_{\text{c.m.}} \approx 59^\circ$ and 64° are omitted because of relatively large regions where data was not obtained. The low energy forward-angle omissions in Fig. 4 are due to overlap in the ^8Be energy spectra with yield from the $^{12}\text{C}(^{12}\text{C}, ^8\text{Be})^{16}\text{O}$ reaction.

There are several structures in Figs. 2, 3, and 4 which are well correlated in energy at many observation angles and in two or more reaction channels. The most prominent structure in all three figures is observed at approximately 16.70 MeV. In this same energy region there are also well defined enhancements near 15.62, 16.30, and 17.30 MeV, plus a weak shoulder effect near 17.0 MeV which is more pronounced in Fig. 4; whereas in Figs. 2 and 3 it is often obscured by the strength of the 16.70 MeV structure. The resonance near 17.30 MeV is particularly interesting because it is so small, yet it is consistently displayed over a broad angular range in all three channels. The cross sections in the 12 to 15 MeV region are very complex with the most prominent structures occurring near 13.80 and 14.25 MeV. Below 13 MeV, although considerable structure appears in the ground state data, there are no compelling correlations.

The angle summed cross sections have been calculated using the equation

$$\sigma_{\text{sum}} = \sum_{i=1}^N \sigma(\theta_i) \sin\theta_i. \quad (1)$$

The summation is over as many as 38 angles from $\theta_{\text{c.m.}} \approx 12^\circ$ – 167° in $\sim 4^\circ$ intervals. Since the angular full width at half maximum (FWHM) of the detection efficiency is approximately 2° ($\sim 3^\circ$ to 4° c.m.) the use of Eq. (1) yields a fairly accurate determination of the relative total cross sections when the full angular range of data is available. Results of this summation applied to the 0^+ , 2^+ , and 4^+ exit channels are shown in Fig. 5, where the angular ranges over which the summations were carried out are also indicated. The small vertical arrows indicate energies at which the number of the terms in the summation changes. For the ground state data all 38 angles are included above ~ 13.3 MeV; from ~ 11.9 to 13.3 MeV the angles $\sim 59^\circ$ and $\sim 64^\circ$ are omitted; and below 11.9 MeV the additional angles near 51° and 55° are omitted from the summation. For the 2^+ channel, data from two back angles, $E_{\text{c.m.}} < 13.3$ MeV, and

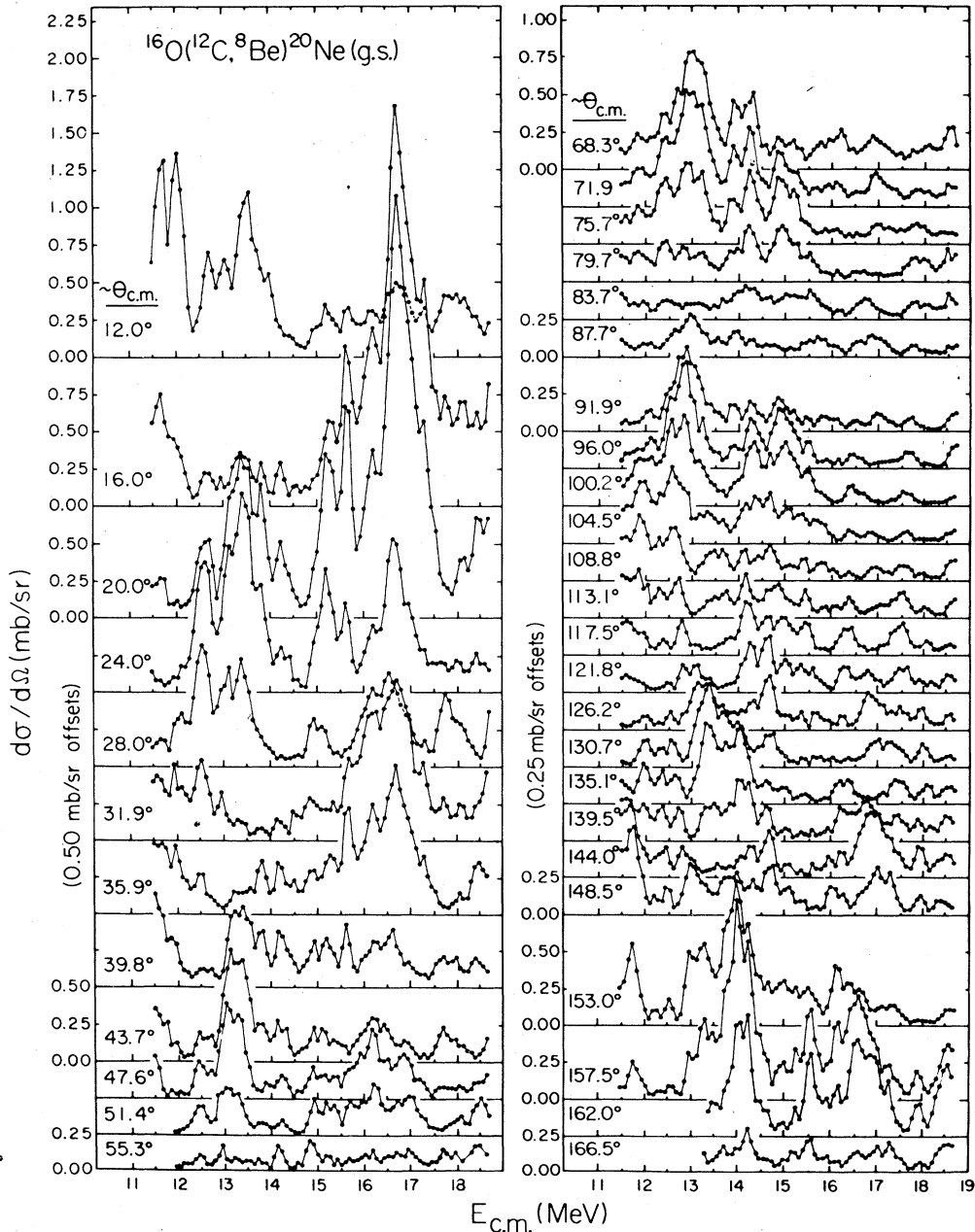


FIG. 2. Excitation function for the reaction $^{16}\text{O}(^{12}\text{C}, ^8\text{Be})^{20}\text{Ne}(0^+)$ measured for 36 angles, $E_{c.m.} \approx 11.5\text{--}18.6$ MeV.

from several intermediate angles at various energies, as seen in Fig. 3, have not been included. The summation for the 4^+ channel includes all data from Fig. 4 for $\theta_{c.m.} > 86^\circ$.

As expected from Figs. 2, 3, and 4, the most consistently prominent structure in Fig. 5 is again at 16.70 MeV although many structures well correlated in energy appear in all channels. It is interesting to note that the structures near 17.7 and 18.0 MeV, so prominent in the 2^+ and 4^+ channels, respectively, are almost nonexistent in the

σ_{sum} for the 0^+ channel. However, close inspection of Fig. 2 shows that both anomalies are present and the 18.0 MeV structure is very well isolated at back angles, where, as we shall see later, it has a well defined oscillatory angular distribution.

Criteria for the identification of structures in excitation functions as resonances have been presented by a number of authors.^{2,5,6} The criteria adopted for use on the present data are similar to those of our previous work² and they are briefly stated as follows:

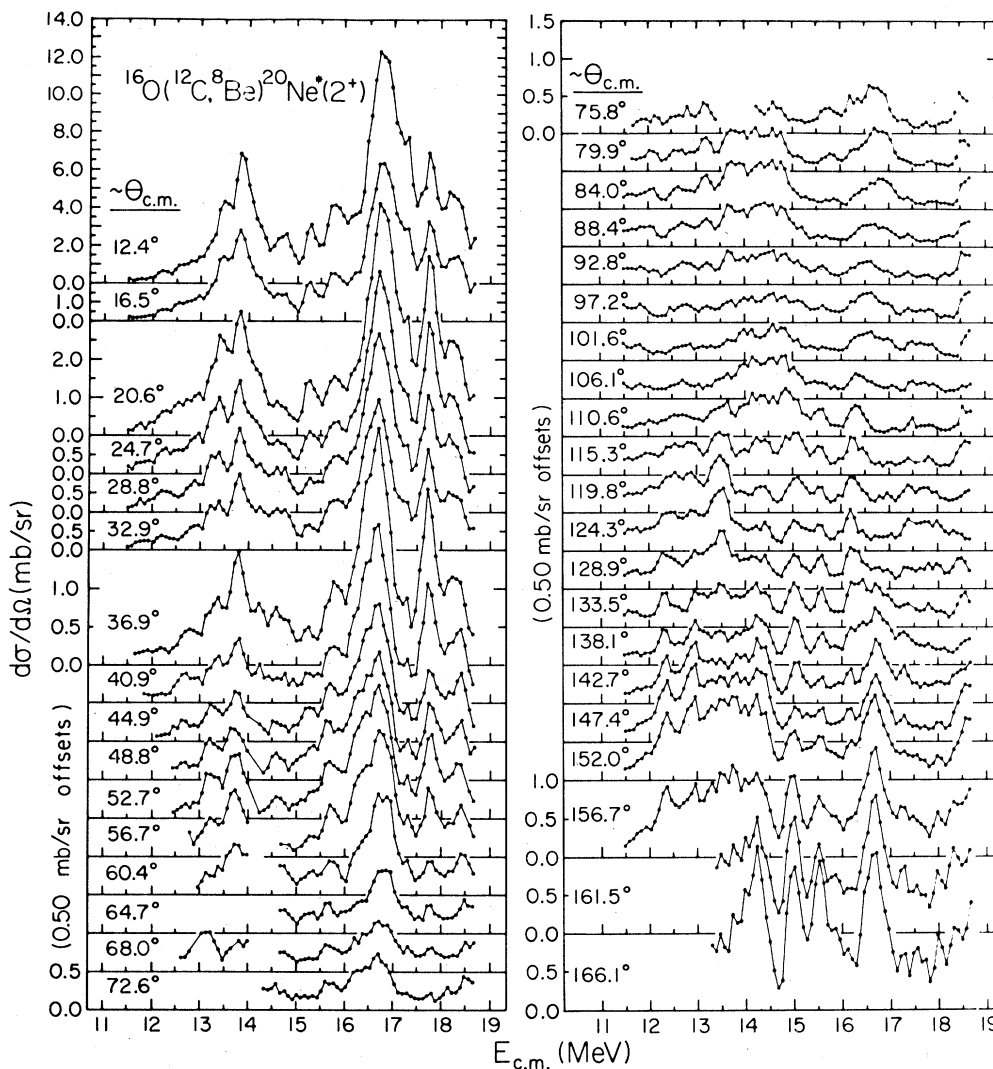


FIG. 3. Excitation functions for the reaction $^{16}\text{O}(^{12}\text{C}, ^8\text{Be})^{20}\text{Ne}^*(2^+)$ measured for 37 angles, $E_{c.m.} \approx 11.5\text{--}18.6$ MeV.

(a) A resonance is observed in a particular reaction channel when it can be identified in the excitation functions over an angular range much greater than the coherence angle.

(b) A resonance must appear as a maximum in the total cross section for two or more reaction channels and the resonance energy is taken from positions of these maxima. Clearly, if an anomaly is observed in the total cross section for a particular channel, then one would expect it to appear over a broad angular range in that channel. However, the reverse is not necessarily true; a weak resonance may appear clearly at many widely separated angles, without being strong enough to survive as a discernable maximum in the total cross section. Therefore, satisfaction of criterion (a)

does not automatically lead to satisfaction of criterion (b), but it can be used to corroborate resonances which do not fully satisfy criterion (b), and thereby result in tentative resonance identifications.

For the purpose of imposing criterion (b), we use the summed cross sections of Fig. 5 as total cross sections. This is a fairly accurate approximation for the 0^+ and 2^+ channels, although in the case of the 4^+ channel only $\theta_{c.m.} > 85^\circ$ are included. Also, only the 0^+ , 2^+ , and 4^+ channels are considered, since although the cross sections to the $3^-, 1^-$ doublet do show correlated resonantlike behavior, it is not as well developed as in the other channels. In the case of the ground state, the total cross section is also formed from values of the zero

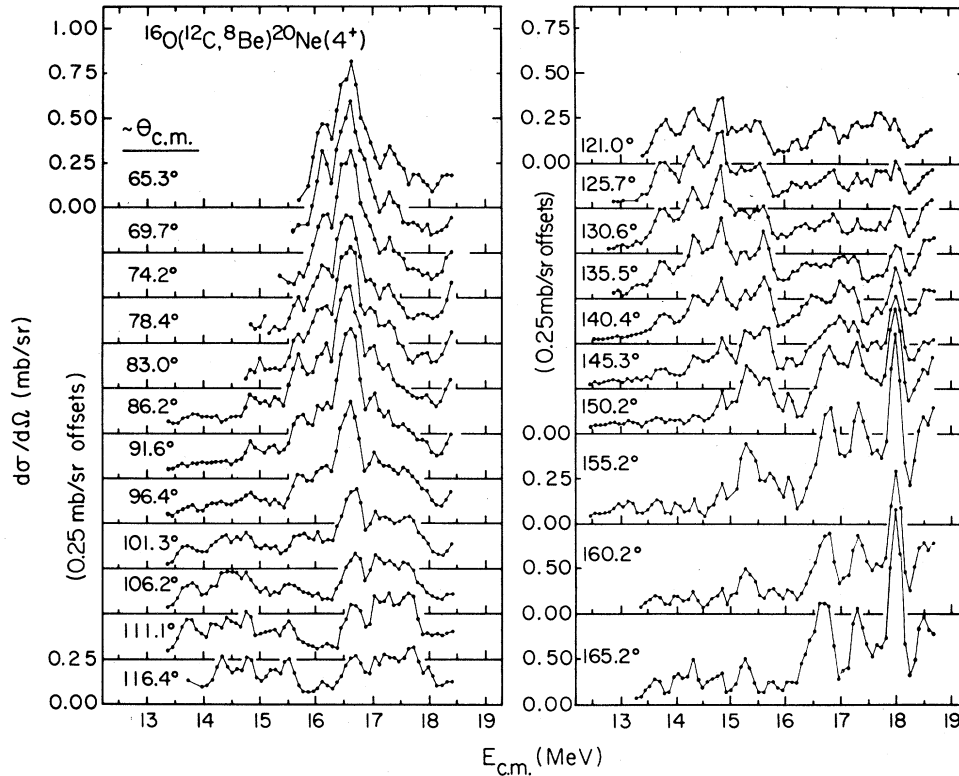


FIG. 4. Excitation functions for the reaction $^{16}\text{O}(^{12}\text{C}, ^8\text{Be})^{20}\text{Ne}(4^+)$ measured for 22 angles, $E_{\text{c.m.}} \sim 13\text{--}18.6$ MeV.

order coefficients in the fitted expansion

$$\sigma(\theta, E) = \sum_{k=0}^{2l} a_k(E) P_k(\cos\theta), \quad (2)$$

where $\sigma_{\text{tot}}(E) \equiv 4a_0(E)$. The coefficients are discussed in greater detail in Sec. III B.

The resonance energy information resulting from application of criteria (a) and (b) to the data of Figs. 2–5 is given in Table I. The energies in parentheses in column one are those of possible resonances not clearly established in this work since criterion (b) is not satisfied. Most of the other resonances are seen in the σ_{sum} of all three reaction channels. The most reliable resonance energies of 13.80, 14.25, 15.62, 16.20, 16.70, 17.30, 17.98, and 18.55 MeV are assigned an estimated probable error of 50 keV. Other resonance energies listed may be in error by 100 keV. The widths of the resonances are mere estimates and errors may be 20% or larger. The J^π information listed in Table I is discussed in Sec. III B. The qualitative relative strengths of the structures in the three separate channels are also indicated in Table I.

The summed cross section excitation functions of Fig. 5 do not extend over the 18.55 MeV resonance because of some missing data at intermediate

angles. This resonance is illustrated in the summed cross sections of Fig. 6, where for the ground state reaction channel we have separately constructed σ_{sum} for ranges of forward, middle, and backward angles. The back-angle distributions are analyzed for resonant J^π values in Sec. III B, and Fig. 6 also shows that σ_{sum} maximizes on resonance in the angular range analyzed, although the peak to valley ratio is much less than at individual angles selected to favor resonant l values (see Fig. 2).

B. Angular distributions and J^π assignments

The angular distributions of the ^8Be exit channel leading to the $^{20}\text{Ne}(0^+)$ ground state are particularly useful in establishing the dominant l values at a resonance energy, since the cross section can be expressed as

$$\sigma(\theta, E) = \left| \sum_{l=0}^L A_l(E) e^{i6l(\theta)} P_l(\cos\theta) \right|^2, \quad (3)$$

and only one term in this coherent summation resonates. Although it is not possible to uniquely extract the complex Legendre coefficients of Eq. (3), the dominant l values can often be obtained by a comparison of the measured angular distribution on resonance with a single term of Eq. (3).

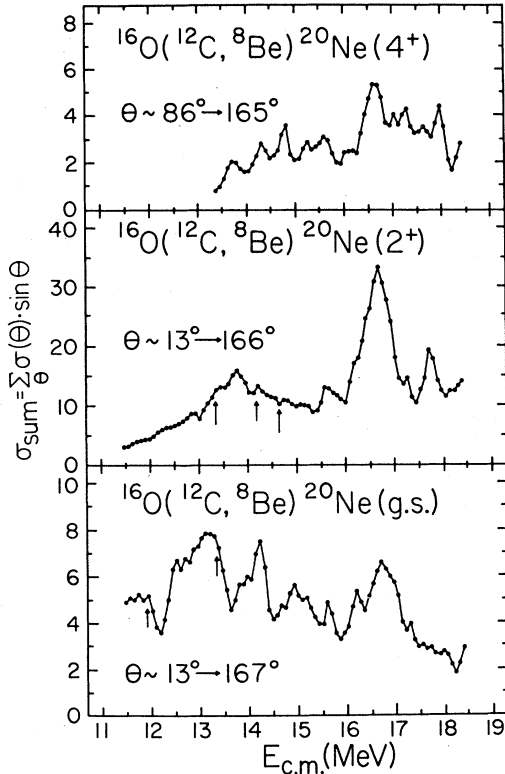


FIG. 5. Angle summed cross sections for the exit channels with $J^\pi(\text{Ne}) = 0^+, 2^+, \text{ and } 4^+$, by use of Eq. (1) in the text. Angular ranges for summations are indicated.

Implied is the assumption that other coefficients are small by comparison. For the $(^{12}\text{C}, ^8\text{Be})$ reaction that assumption is more nearly correct when considering $\sigma(\theta)$ in a back-angle region, where the direct alpha-particle transfer component of the cross section is largely absent.

Comparisons between measurements for $\theta > 100^\circ$ and the functions $P_l^2(\cos\theta)$ are presented in Fig. 7 for $E_{c.m.}$ values near the nine proposed resonances of Table I which have the most definitive J^π assignments. Six of these are also among the most well defined in energy from Figs. 2–6. These six resonances, $E_{c.m.}, J^\pi = 13.80 \text{ MeV}, 8^+; 14.25 \text{ MeV}, 9^-; 16.70 \text{ MeV}, 10^+; 17.30 \text{ MeV}, 12^+; 17.98 \text{ MeV}, 11^-; \text{ and } 18.55 \text{ MeV}, 10^+$, must then be considered those most reliably established in this work.

In two cases where a weak resonance is near a much stronger one, a fitting function also used is $W(\theta) = a_1 P_{l_1}^2 + a_2 P_{l_2}^2$, where $|l_1 - l_2| = 1$. This is merely a fitting parametrization to illustrate the shift in the measured angular position of back-angle maxima in $\sigma(\theta)$ and is not to be confused with any sort of approximation for Eq. (3). Any approximation to Eq. (3) would require what is probably a strong interference term. Such an

TABLE I. Resonances in $^{16}\text{O}(^{12}\text{C}, ^8\text{Be})^{20}\text{Ne}^*$.^a

$E_{c.m.}^b$ (MeV)	Relative presence in ^{20}Ne (J^π) final state ^c			$\Gamma_{c.m.}^d$ (keV)	$E_x(^{28}\text{Si})$ (MeV)	J^π
	0^+	2^+	4^+			
(11.8)	m	<650	28.6	$(6^+, 7^-)$
(12.5)	m	w		420	29.3	$(7^-, 8^+)$
(12.8)	m	w		<500	29.6	...
(13.1)	w	w		<500	29.9	7^-
13.3	m	m		500	30.1	8^+
13.80	m	m	m	470	30.55	8^+
(14.0)	w	w	...	350	30.8	$(8^+, 9^-)$
14.25	s	w	m	400	31.00	9^-
14.7	w	w	...	300	31.5	...
14.9	m	...	s	500	31.7	(8^+)
15.2	w	w	m	430	32.0	...
15.62	m	m	m	300	32.37	(10^+)
16.20	s	w	m	470	32.95	$9^-(10^+)$
16.70	s	s	s	700	33.45	10^+
(17.0)	w	w	w	<500	33.8	11^-
17.30	w	w	m	260	34.05	12^+
17.7	w	s	w	500	34.5	(>12)
17.98	w	...	s	260	34.73	11^-
18.55	m	w	w	400	35.30	10^+

^a Present work only.

^b Resonance energies quoted to 10 keV have an estimated probable error ≤ 50 keV. Those in parentheses are not well established resonances in the present data. Others have an estimated probable error of ~ 100 keV.

^c s(strong), m(medium), w(weak), ... (not observed).

^d Probable errors on width estimates are $\sim 20\%$.

interference term could be evaluated properly only if the entire angular range is considered, which would then include direct contributions and introduce unwanted complications into the fitting procedure. These two cases are listed in Table I at $E_{c.m.} = 13.1$ and 17.30 MeV and nearby angular distributions are shown in Fig. 7. The results of this parametrization of back-angle data in the two energy regions are shown in Fig. 8. In the two cases the positions of maxima in $\sigma(\theta)$ tend toward those for $l=7$ and $l=12$, respectively, as energy is increased through the resonance. The structure near 13 MeV is not well established in this work as indicated in Table I although it shows prominently at many angles in the ground state data of Fig. 2. The resonance at 17.30 MeV is, however, unmistakable as it appears over a broad range of angles and in the total cross sections for all three channels.

The $J^\pi = 12^+$ assignment for the 17.30 MeV resonance is by no means without the remote possibility of error. The shift evident in Fig. 8 certainly indicates $l_{\text{res}} \neq 11$ and a resonant contribution from $l < 11$ would require a most unusual interference with the $l=11$ background to produce the result shown in Fig. 8. If $l_{\text{res}} \geq 13$ it would be the

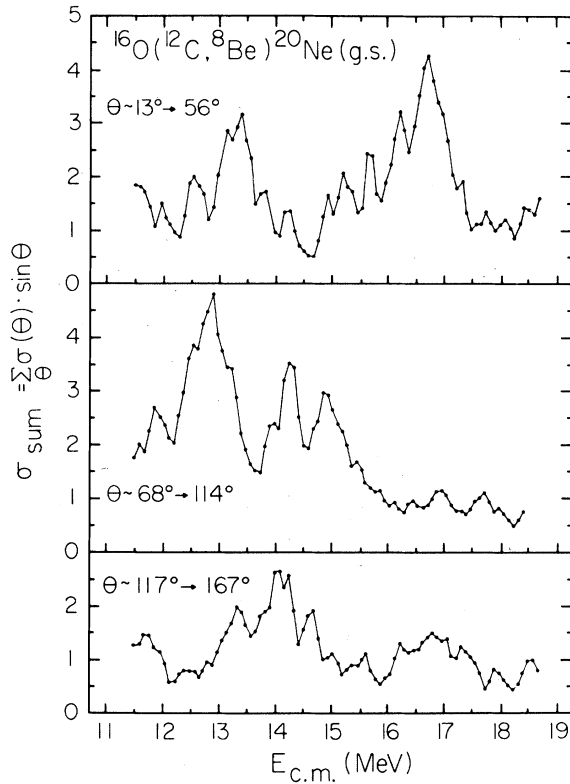


FIG. 6. Angle summed cross sections for the $^{16}\text{O}(^{12}\text{C}, ^8\text{Be})^{20}\text{Ne}(\text{g.s.})$ reaction. The summation is performed separately for angular ranges of forward, intermediate, and back angles as indicated.

only example of a heavy ion resonance to lie outside the grazing angular momentum. Even with the present assignment the 17.30 MeV resonance is the lowest energy 12^+ reported to date, and the lowest 13^- lies at $E_{\text{c.m.}} \approx 20.9$ MeV.²

One would hope to gain considerable insight toward establishing resonance J^π values by observing the k dependence of the coefficients $a_k(E)$ of Eq. (2), evaluated on and off resonance, since the value of $a_k(E_{\text{res}})$ should maximize at $k = 2l_{\text{res}}$ with small values of a_k for $k > 2l_{\text{res}}$ arising only from interference effects. The coefficients have been evaluated for all ground state angular distributions for data sets covering the entire angular range, the forward angles only, and the backward angles only. In the latter two cases only even values of k are used in Eq. (2). Although supportive of spin assignments in most cases, the behavior of values of a_k vs k does not provide us with information more compelling than the simple comparisons with $P_l^2(\cos\theta)$. In fact, due to the uncertainties in extracted values of the coefficients, the spin information is often less convincing. These uncertainties arise due to the very large number of terms needed to fit the data

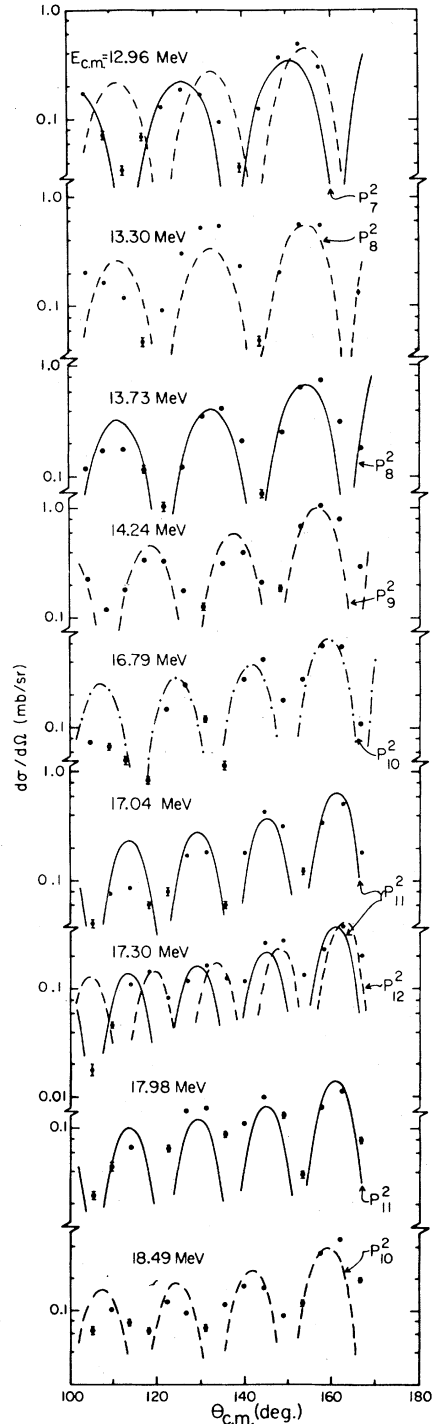


FIG. 7. Back-angle angular distributions for the reaction $^{16}\text{O}(^{12}\text{C}, ^8\text{Be})^{20}\text{Ne}(0^+)$ at energies near the prominent resonances of Table I. The curves are nearest fit $P_l^2(\cos\theta)$ functions.

and the present lack of data within 10° of the beam axis. The problem of extracting reliable coefficients is most severe at the lower energies, due to more restricted data.

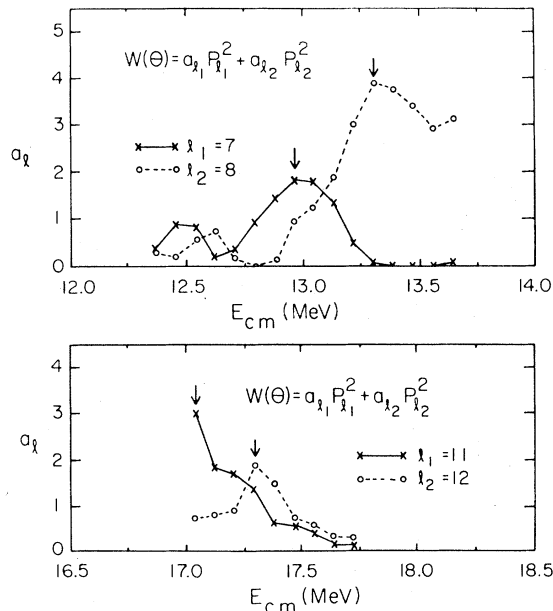


FIG. 8. Amplitudes, a_l , obtained by fitting the data with a sum of two $P_l^2(\cos\theta)$ functions illustrating the shifts in oscillatory patterns of $\sigma(\theta)$ near 13.0 and 17.3 MeV. Arrows indicate the energies for which back angle $\sigma(\theta)$ is shown in Fig. 7.

For the ground state channel the zero order coefficient and hence the total cross section is obtained reliably by performing fits to the data using Eq. (2) and increasing $2L$ until $a_0(E)$ becomes nearly constant vs $2L$. The energy dependence of the coefficient $a_0(E)$ is shown in Fig. 9. The upper portion of the figure, proportional to

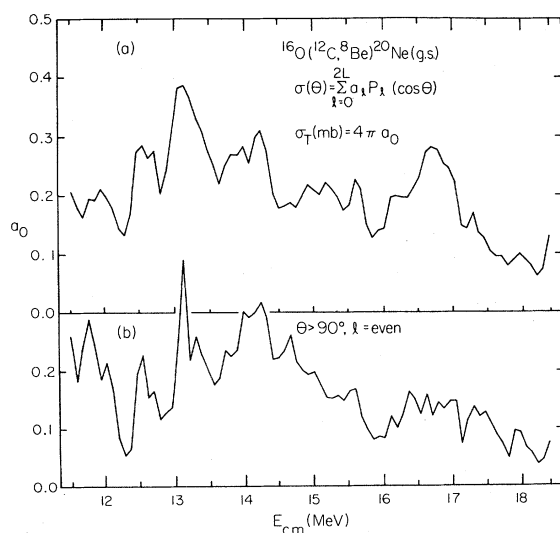


FIG. 9. Energy dependence of the zero order Legendre coefficients from fitting Eq. (2) to the ground state data. (a) Full angular range, all k values, (b) back angles only, $k = \text{even}$.

the total cross section, is very similar in structure to the summed cross section data of Fig. 5, for $E_{c.m.} > 13$ MeV. Below 13 MeV the values of $a_0(E)$ are less well determined because of less complete angular distributions, and this most likely accounts for the differences in Figs. 5 and 9 in this energy region. The values extracted from back-angle data only (lower part of Fig. 9) might be expected to show the resonance structure more clearly since the direct reaction contribution is small at back angles. Although some differences are evident between the two curves, a significantly more vivid picture of resonant structures is not obtained.

Another convincing characteristic of resonance behavior is the change in the angular distribution through the resonance energy. Figure 7 displays angular distributions on resonance only and clearly the illustration of the energy dependence of angular distributions through all the resonances of Table I would be too lengthy. The weak resonance at $E_{c.m.} = 17.98$ MeV is chosen to illustrate the behavior of the angular distributions through a resonance, since it is relatively isolated in the back-angle excitation functions. Shown in Fig. 10, these data display a narrow and well developed $l = 11$ enhancement for $\theta > 100^\circ$ with relatively little signature of a resonance at the forward angles. In fact the cross section on the forward maximum of Fig. 10 diminishes slightly at the resonance energy, due presumably to interference with the direct contribution (see also Fig. 3). Because of the large nonresonant component at forward angles,

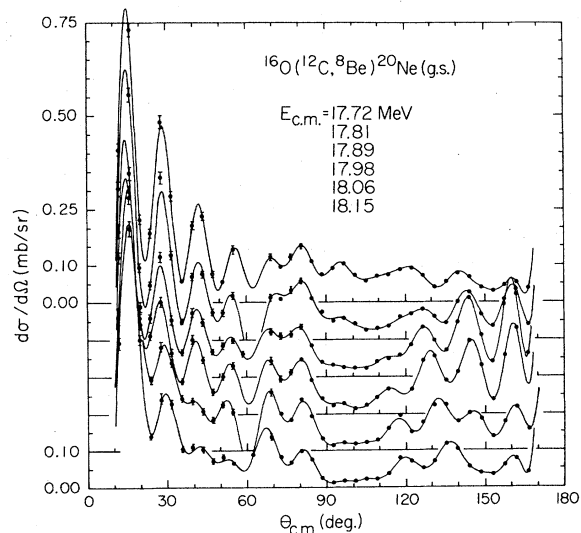


FIG. 10. Complete angular distributions for $^{16}\text{O}(^{12}\text{C}, ^8\text{Be})^{20}\text{Ne}$ through the resonance near $E_{c.m.} = 18$ MeV. Error bars reflect statistical errors in data extraction only. The solid curves are generated by fitting the Legendre expansion of Eq. (2) to experimental data.

the overall effect in the ground state summed cross section is extremely weak; however, the existence of the resonance is strongly supported by the 4^+ data of Figs. 4 and 5.

It is clear that the forward-angle cross sections at these energies (Fig. 10) are dominated by a reaction mechanism which is different from that producing the back-angle yield simply from the more rapid oscillations and the lack of significant change in forward-angle cross sections over the resonance. This effect is quantified by performing a Legendre analysis of the forward and backward angular regions independently, using only even terms in Eq. (2). The result is displayed in Fig. 11 as total χ^2 per degree of freedom versus the maximum order in the fitted Legendre expansion. It is evident that the partial waves dominant at forward angles are two to three units greater than the dominant $l=11$ ($2L=22$) of this resonance. The sum effect is observed at the 16.70 MeV, 10^+ and the 18.55 MeV, 10^+ resonances. We interpret this difference as a difference in the mean interaction distance for the direct alpha-particle transfer reaction and the heavy ion resonance formation of $^{28}\text{Si}^*$, both of which are considered surface reactions. Using $l=kr$, these mean distances are the order of 6 and 7 fm for $l=11$ and $l=13$, respectively. Classically the c.m. separation of $^8\text{Be} + (^{16}\text{O} + \alpha)$ system in surface contact is 7.1 fm, whereas for the $^{16}\text{O} + ^{12}\text{C}$ system it is 6.4 fm, using $r_0 = 1.34$ fm.

IV. DISCUSSION AND COMPARISON

A number of structures have been identified as resonances in the previous section and in many cases the dominant l value is determined. Fur-

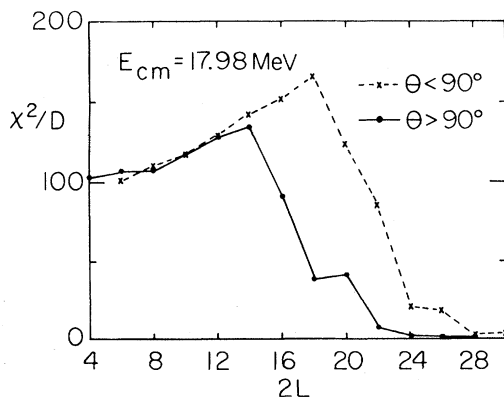


FIG. 11. The value of χ^2 per degree of freedom vs $k_{\max} = 2L$ when fitting forward and back-angle $\sigma(\theta)$ with Eq. (2) with even order polynomials only. The increasing value of χ^2/D for low increasing values of $2L$ is due to a decreasing number of degrees of freedom without corresponding improvement in χ^2 .

ther support for their resonance character can be obtained from a comparison with the structures observed in other reaction channels, their energies, and when available, the J^π values. Information from the major resonance investigations in the energy region $E_{\text{c.m.}} = 11.5\text{--}18.6$ MeV is summarized in Fig. 12. The dashed lines connecting energy levels indicate possible correspondences which are discussed in the following paragraphs.

In the c.m. energy region below 13 MeV we report resonances at 11.8 and 12.5 MeV although the evidence presented in Fig. 9 indicates that each of these could be doublets with energies of 11.8, 12.0, 12.5, and 12.7 MeV. This region has also been studied for the proton exit channel by Lumpkin *et al.*⁷ with equally confusing results. They observe strong maxima in the $\theta_L = 10^\circ$ yields at $E_{\text{c.m.}} = 11.0, 11.8,$ and 12.5 MeV for the $^{27}\text{Al}^*$ ($E_x = 4.51$ MeV) final state and at $E_{\text{c.m.}} = 11.4$ and 12.0 MeV for the $E_x = 3.00$ final state. A number of authors⁸⁻¹⁰ have reported a resonance at 12.8 MeV with $J^\pi = 7^-$. The conclusion of Disdier *et al.*⁹ is based on ^8Be (g.s.) angular distributions similar to the present data. It is important to note that not only can we not assign a J^π value on the basis of the criteria employed here, but there is absolutely no evidence for a resonance in the ground state total cross section at 12.8 MeV (see Fig. 9). The summed cross section values of Fig. 5 show only

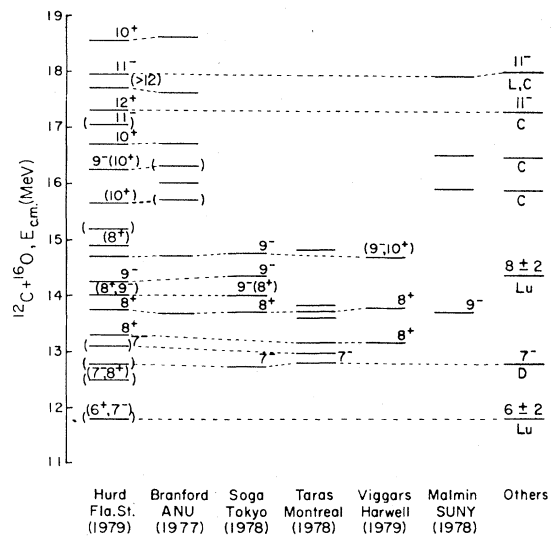


FIG. 12. Comparison of published resonance information for $^{12}\text{C} + ^{16}\text{O}$, $E_{\text{c.m.}} = 11.5\text{--}18.6$ MeV. References are as follows: Hurd (present work), Branford (Ref. 13), Soga (Ref. 8), Taras (Refs. 10 and 11), Viggars (Ref. 14), and Malmin (Ref. 16). The designations in the right-hand column are as follows: L (Lee *et al.*, Ref. 17), C (Charles *et al.*, Ref. 15), Lu (Lumpkin *et al.*, Ref. 7), and D (Disdier *et al.*, Ref. 9).

a very weak effect at this energy. The discrepancy between Figs. 5 and 9 is again due to the inability to obtain good values from Eq. (2) when small but important angular ranges of data are unavailable.

The fine structure reported by Taras *et al.*¹¹ for the total gamma-ray yield is reproduced in part by our results in the 13 to 14 MeV region. The 12.97 MeV resonance corresponds to our 7⁻ resonance at 13.1 MeV, the energy of which is quoted on the basis of Fig. 9 rather than Figs. 7 and 8, which would indicate something much closer to 12.97 MeV as reported earlier.¹² The two anomalies near 13.0 and 13.3 MeV are clearly indicated in a number of the yield curves; for example, $\theta_{c.m.} = 153^\circ, 157.5^\circ$ for the ground state data (Fig. 2). The triplet of structures¹¹ near 13.60, 13.69, and 13.81 MeV has only one identifiable member in the present work which probably also corresponds with the 13.7 MeV anomaly observed in gamma-ray yields by Branford *et al.*,¹³ the 13.7 MeV, 8⁺ assignment of Soga *et al.*,⁸ and the 13.77 MeV, 8⁺ assignment of Viggars *et al.*¹⁴ The other result of Viggars, and 8⁺ resonance at 13.15 MeV, is not acceptable in light of the present data, since it is based on the analysis of an estimated total cross section for the $^{12}\text{C}(^{16}\text{O}, ^{20}\text{Ne g.s.})^8\text{Be}$ reaction which bears little resemblance to the actual cross sections shown in Fig. 5. The structures observed near $E_{c.m.} = 14.0, 14.25,$ and 14.7 MeV (see Table I) are also reported by Soga *et al.*⁸ and the spin determinations are compatible. The present work indicates a doublet, 14.7 and 14.9 MeV, which is not supported by any other experiment although reported single resonance energies in this region range from 14.7 MeV (Refs. 13 and 14) to 14.83 MeV.¹¹

The only resonances clearly identified between 15 and 17 MeV in the present work, $E_{c.m.} = 15.62, 16.20,$ and 16.70 MeV, are also observed in the gamma-ray yields of Branford *et al.*,¹³ which of course include gamma rays from the $^{16}\text{O}(^{12}\text{C}, ^8\text{Be})^{20}\text{Ne}^*$ reactions. These observations are not in agreement with the resonances reported in elastic¹⁵ and inelastic¹⁶ scattering of $^{12}\text{C} + ^{16}\text{O}$, near 15.9 and 16.5 MeV. The resonance in this ⁸Be work at $E_{c.m.} = 16.70$ MeV is the most dominant structure observed in the yields for all exit channels and cannot be confused with the resonance near 16.5 MeV observed in elastic and inelastic scattering.^{15,16} The resonance at 17.3 MeV was also observed very clearly in the back-angle elastic scattering by Charles *et al.*,¹⁵ who assigned a spin of 11⁻. The J value of the resonance is quite unmistakably $\neq 11$ based on the data of Figs. 7 and 8 from which we assign $J^\pi = 12^+$. The $J^\pi = 11^-$ result from the back-angle elastic scattering is highly dependent on the assumption that the back-

ground amplitudes for all l values may be described by a standard optical potential of Woods-Saxon shape. Since the off-resonance back-angle scattering of $^{12}\text{C} + ^{16}\text{O}$ is much too strong to be consistent with this assumption, it is likely that the background amplitudes are quite different from those assumed in such an analysis.

The remaining three resonances have all been observed elsewhere.^{13,15,17,18} The 17.7 MeV resonance, which may have $J > 12$ because of its absence in the ground state and strong presence in the 2⁺ channel, and the 18.55, 10⁺ were also observed in gamma-ray yields at 17.6 and 18.6 MeV by Branford *et al.*¹³ and at 17.71 and 18.57 MeV by Kolata *et al.*¹⁸ The reports by Branford^{13,19} that there exists a resonance doublet at 18.6 and 18.8 MeV are apparently borne out by observation of 10⁺ structures at the present 18.55 MeV, and other ⁸Be work reporting resonances at 18.8 MeV (Ref. 20) and 18.87 MeV.² The very well defined $J^\pi = 11^-$ resonance at 17.98 MeV discussed earlier (Fig. 10) has also been observed in the elastic¹⁵ and inelastic¹⁶ scattering without J^π assignment. The present work confirms an earlier assignment by S. M. Lee.¹⁷

The 18.8 MeV, 10⁺ has been cited by Eberhart *et al.*²⁰ as lying deep within the region of strong absorption as ascertained by the trajectory of l_{\max} values extracted from total fusion cross sections on a plot of $E_{c.m.}$ vs J (see Fig. 3, Ref. 20). The only other resonance to lie within this region was the 17.30 MeV, 11⁻ observed by Charles *et al.*¹⁵ However, the present work shows quite clearly that $J \neq 11$ for that resonance. The present work, however, now places several other resonances within the strong absorption l_{\max} such that the entire region between the 18.8 MeV, 10⁺ resonance and the l_{\max} locus²⁰ is now virtually filled in by the assignments of Table I and Fig. 12 by the resonances with $J^\pi = 9^-$ at $E_{c.m.} = 14.25, 14.7,$ and 16.2 MeV; $J^\pi = 10^+$ at $E_{c.m.} = 16.7$ and 18.55 MeV; and $J^\pi = 11^-$ at $E_{c.m.} = 17.0$ and 17.98 MeV along with the earlier report by James² of a weak 11⁻ resonance at 19.15 MeV, although none is so deeply embedded as the 18.8 MeV, 10⁺.

A compilation of resonances in the $^{12}\text{C} + ^{16}\text{O}$ system, $E_{c.m.} = 11$ to 23 MeV, observed through the variety of exit channels which have provided J^π information is shown in Fig. 13 (see figure for references). The grazing angular momentum indicated is for an entrance channel optical model.^{16,20} The ⁸Be exit channel grazing angular momentum is approximately two units less for the same entrance channel $E_{c.m.}$. It seems to be the general result that J values determined and cited in the present work are from one to three units less than

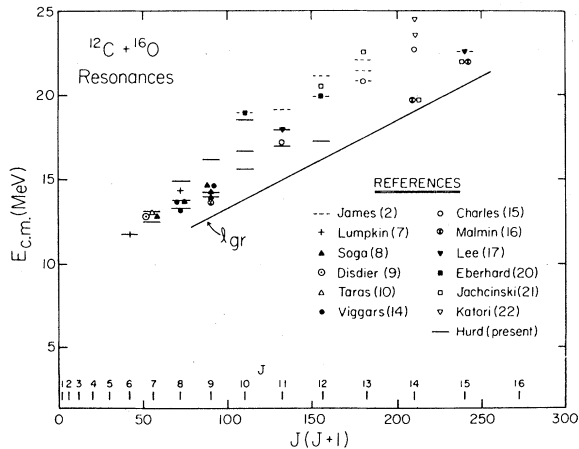


FIG. 13. Positions of known $^{12}\text{C} + ^{16}\text{O}$ resonances, $E_{c.m.} = 11\text{--}25$ MeV, relative to the optical model grazing angular momentum.

optical model or strong absorption expectations. Spin sequences, such as those suggested by Branford *et al.*,¹³ Resmeni *et al.*,²³ and Golin,²⁴ with optical model considerations or $J(J+1)$ systematics in mind have resulted in speculative J assignments which are too large when compared to present experimental results and therefore these sequences are not acceptable.

This result is consistent with our interpretation

of the data of Figs. 10 and 11, which says that at $E_{c.m.} \sim 18$ MeV the grazing angular momentum for direct alpha-particle transfer exceeds the value of l_{res} by approximately two units, in spite of the fact that both effects are observed via the ^8Be exit channel. It is therefore implied that heavy ion resonances do indeed occur deep within the optical model strong absorption region and although a generally smaller exit channel grazing l would tend in that direction it does not account for the result. The conflict between the necessity of small absorption for observable resonances and their location within a supposed strong absorption region is not understood.

ACKNOWLEDGMENTS

The quantity of data involved in this work required the assistance of many individuals in addition to the authors. We acknowledge the experimental work of Dr. Don James, Dr. Alex Lumpkin, Dr. Larry Medsker, and especially Dr. Amit Roy; assistance with data reduction from Norbert Hoernschemeyer and Calvin Stubbins; and the computer and accelerator expertise provided by Dr. Joe Johnson, Dr. Russell LeClaire, and Dr. Ken Chapman. This work was supported in part by the National Science Foundation.

*Present address: Department of Physics, University of Pennsylvania, Philadelphia, Pa. 19174.

†Present address: Department of Physics, Tennessee Technological University, Cookeville, Tenn. 38501.

¹R. G. Stokstad, D. Shapira, L. Chua, P. Parker, M. W. Sachs, R. Wieland, and D. A. Bromley, *Phys. Rev. Lett.* **28**, 1523 (1972); R. E. Malmin, R. H. Siemssen, D. A. Sink, and P. P. Singh, *ibid.* **28**, 1590 (1972); E. R. Cosman, A. Spurduto, T. M. Cormier, T. N. Chin, H. E. Wegner, M. F. Levine, and D. Schwalm, *ibid.* **29**, 1341 (1972).

²D. R. James and N. R. Fletcher, *Phys. Rev. C* **20**, 560 (1979).

³G. R. Morgan and N. R. Fletcher, *Phys. Rev. C* **16**, 167 (1977).

⁴J. G. Cramer, K. A. Eberhard, N. R. Fletcher, E. Mathiak, H. H. Rossner, and A. Weidinger, *Nucl. Instrum. Methods* **111**, 425 (1973).

⁵P. Taras, in *Clustering Aspects of Nuclear Structure and Nuclear Reactions, Winnipeg, 1977*, Proceedings of the Third International Conference on Clustering Aspects of Nuclear Structure and Nuclear Reactions, edited by W. T. H. Van Oers, J. P. Svenne, J. S. C. McKee, and W. R. Falk (AIP, New York, 1978), p. 234.

⁶H. Voit, W. Galster, W. Treu, H. Frölich, and P. Dück, *Phys. Lett.* **67B**, 399 (1977).

⁷A. H. Lumpkin, G. J. KeKelis, K. W. Kemper, and

A. F. Zeller, *Phys. Rev. C* **13**, 2564 (1976).

⁸F. Soga, J. Shimizu, H. Kamitsubo, N. Takahashi, K. Takimoto, R. Wada, T. Fujusawa, and T. Wada, *Phys. Rev. C* **18**, 2457 (1978).

⁹D. Disdier, B. Haas, S. M. Lee, J. C. Merdinger, V. Rauch, F. Scheibling, Y. Schutz, M. Toulemonde, and J. P. Vivien, see Ref. 5, p. 590.

¹⁰P. Taras and G. R. Rao, *Phys. Rev. C* **19**, 1557 (1979).

¹¹P. Taras, G. R. Rao, and G. Azuelos, *Phys. Rev. Lett.* **41**, 840 (1978).

¹²Florida State University Tandem Laboratory Annual Report, 1979, p. 57 (unpublished).

¹³D. Branford, B. N. Nagorcka, and J. O. Newton, *J. Phys. G* **3**, 1565 (1977).

¹⁴D. A. Viggars, T. W. Conlon, F. P. Brady, and I. Naqib, *Phys. Rev. C* **19**, 2186 (1979).

¹⁵P. Charles, F. Auger, I. Badawy, B. Berthier, M. Dost, J. Gastebois, B. Fernandez, S. M. Lee, and E. Plagnol, *Phys. Lett.* **62B**, 289 (1976).

¹⁶R. E. Malmin, J. W. Harris, and P. Paul, *Phys. Rev. C* **18**, 163 (1978).

¹⁷S. M. Lee, in *Proceedings of the INS-IPCR Symposium on Cluster Structure of Nuclei and Transfer Reactions Induced by Heavy Ions, Tokyo, 1975*, edited by H. Kamitsubo, I. Kohno, and T. Marumori (The Institute of Physical and Chemical Research, Wako-shi, Saitama, Japan, 1975), p. 285.

- ¹⁸J. J. Kolata, R. M. Freeman, F. Haas, B. Heusch, and A. Gallman, Phys. Rev. C 19, 408 (1979).
- ¹⁹D. Branford, J. O. Newton, J. V. Robinson, and B. N. Nagorcka, J. Phys. A 7, 1193 (1974).
- ²⁰K. A. Eberhard, H. Bohn, and K. G. Bernhardt, Phys. Rev. Lett. 42, 432 (1979).
- ²¹C. M. Jachcinski *et al.*, private communication.
- ²²K. Katori, K. Furuno, and T. Ooi, Phys. Rev. Lett. 40, 1489 (1978).
- ²³F. G. Resmini, F. Soga, and H. Kamitsubo, Phys. Rev. C 15, 2241 (1977).
- ²⁴M. Golin, Phys. Lett. 74B, 23 (1978).